Cyclic Alopecia and Abnormal Epidermal Cornification in *Zdhhc13*-Deficient Mice Reveal the Importance of Palmitoylation in Hair and Skin Differentiation

Kai-Ming Liu[1,2], Yi-Ju Chen[3], Li-Fen Shen[1], Amir N.S. Haddad[1,4], I-Wen Song[1,5], Li-Ying Chen[1,6], Yu-Ju Chen[3], Jer-Yuarn Wu[1], Jeffrey J.Y. Yen[1] and Yuan-Tsong Chen[1,2,7]

Many biochemical pathways involved in hair and skin development have not been investigated. Here, we reported on the lesions and investigated the mechanism underlying hair and skin abnormalities in Zdhhc13^{skc4} mice with a deficiency in DHHC13, a palmitoyl-acyl transferase encoded by *Zdhhc13*. Homozygous affected mice showed ragged and dilapidated cuticle of the hair shaft (CUH, a hair anchoring structure), poor hair anchoring ability, and premature hair loss at early telogen phase of the hair cycle, resulting in cyclic alopecia. Furthermore, the homozygous affected mice exhibited hyperproliferation of the epidermis, disturbed cornification, fragile cornified envelope (CE, a skin barrier structure), and impaired skin barrier function. Biochemical investigations revealed that cornifelin, which contains five palmitoylation sites at cysteine residues (C58, C59, C60, C95, and C101), was a specific substrate of DHHC13 and that it was absent in the CUH and CE structures of the affected mice. Furthermore, cornifelin levels were markedly reduced when two palmitoylated cysteines were replaced with serine (C95S and C101S). Taken together, our results suggest that DHHC13 is important for hair anchoring and skin barrier function and that cornifelin deficiency contributes to cyclic alopecia and skin abnormalities in Zdhhc13^{skc4} mice.

Journal of Investigative Dermatology (2015) **135,** 2603–2610; doi:10.1038/jid.2015.240; published online 30 July 2015

INTRODUCTION

Many biochemical pathways involved in hair and skin development have not been investigated. The observation of alopecia and hyperkeratosis in mice with a deficiency in DHHC13, a palmitoyl-acyl transferase (Saleem *et al.*, 2010), prompted us to explore the role of palmitoylation in the skin and hair differentiation.

S-Palmitoylation is a common post-translational modification by which a saturated 16-carbon fatty acid, palmitate (C16:0), is added to specific cysteine residues via thioester linkage. S-Palmitoylation enhances hydrophobicity and generates a membrane anchor, which increases protein affinity for intracellular membranes. Unlike most lipid modifications, protein S-Palmitoylation is reversible. The dynamic modification acts as an on–off switch that regulates several biological mechanisms. Recent studies revealed that S-Palmitoylation modulates protein targeting, trafficking, folding, stability, and protein–protein interactions and is thus involved in endocytosis, cell reproduction and growth, lipid and sugar metabolism, signal transduction of neuronal synapses, and viral infection such as infectivity of HIV-1 and virulence of influenza A virus (Rousso *et al.*, 2000; Charollais and Van Der Goot, 2009; Grantham *et al.*, 2009; Blaskovic *et al.*, 2014).

Palmitoyltransferase (PAT), which mediates protein Palmitoylation, contains an enzymatic core comprising a Asp-His-His-Cys (DHHC) motif within a cysteine-rich domain (Bartels *et al.*, 1999; Roth *et al.*, 2002). Seven DHHC-family PATs have been identified in yeast and 23 in mammals (Fukata *et al.*, 2004; Ohno *et al.*, 2006). PAT substrates include oncoproteins, ion channels, signaling proteins, enzymes, scaffolding proteins, cell adhesion molecules, receptors, and neuronal proteins. Moreover, PAT-substrate specificities have also been demonstrated. For example, PSD-95 is a substrate for DHHC2, 3, 7, and 15; H-Ras and N-Ras are specific substrates of DHHC9

[1]*Institute of Biomedical Sciences, Academia Sinica, Taipei, Taiwan;* [2]*Institute of Clinical Medicine, National Yang-Ming University, Taipei, Taiwan;* [3]*Institute of Chemistry, Academia Sinica, Taipei, Taiwan;* [4]*Department of Biology, University of Toronto Mississauga, Mississauga, Ontario, Canada;* [5]*Graduate Institute of Life Sciences, National Defence Medical Center, Taipei, Taiwan;* [6]*Taiwan Mouse Clinic, National Comprehensive Mouse Phenotyping and Drug Testing Center, Academia Sinica, Taipei, Taiwan and* [7]*Department of Pediatrics, Duke University Medical Center, Durham, North Carolina, USA*

Correspondence: Yuan-Tsong Chen, Institute of Biomedical Sciences, Academia Sinica, 128 Academia Road, Section 2, Nankang, Taipei 11529, Taiwan. E-mail: chen0010@ibms.sinica.edu.tw

Abbreviations: ABE, acyl-biotinyl exchange; CE, cornified envelope; CUH, cuticle of hair shaft; KE, keratin; PND, postnatal day; PAT, palmitoyltransferase; TG, transglutaminase; WT, wild type

Received 25 November 2014; revised 28 May 2015; accepted 16 June 2015; accepted article preview online 29 June 2015; published online 30 July 2015

and 18; and huntingtin (htt) is a specific substrate of DHHC13 and 17 (Huang *et al.*, 2009; Iwanaga *et al.*, 2009). Loss of Palmitoylation in specific PAT substrates is important in the pathogenesis of certain diseases, including Huntington's disease (DHHC13 and 17; Singaraja *et al.*, 2002; Yanai *et al.*, 2006; Singaraja *et al.*, 2011; Milnerwood *et al.*, 2013; Sutton *et al.*, 2013), multiple types of cancers (DHHC2, DHHC9, DHHC11, DHHC14, and DHHC20; Korycka *et al.*, 2012), schizophrenia (DHHC8; Korycka *et al.*, 2012), X-linked mental retardation (DHHC9 and DHHC15; Korycka *et al.*, 2012), acute myeloid leukemia (DHHC14; Yu *et al.*, 2011), type 1 diabetes (DHHC17; Berchtold *et al.*, 2011), and mild hair loss and skin abnormalities (DHHC21; Mill *et al.*, 2009).

We previously reported that Zdhhc13^{skc4} mice (MGI: 2671845) generated through *N*-ethyl-*N*-nitrosourea (ENU) mutagenesis exhibited alopecia, hyperkeratosis, amyloidosis, and osteoporosis (Saleem *et al.*, 2010). We also reported that *Zdhhc13*, a novel regulator, regulates postnatal skeletal development and bone mass acquisition via Palmitoylation of MT1-MMP, thus revealing the role of Palmitoylation in the pathogenesis of human osteoporosis (Song *et al.*, 2014). In this study, we investigated the pathogenic mechanisms of alopecia and skin hyperkeratosis in Zdhhc13^{skc4} mice. First, we studied the changes in morphology, histology, physical properties, and function of the hair and skin. Second, we then investigated the biochemical and molecular basis for these changes and the resulting alopecia and hyperkeratosis.

RESULTS

Cyclic alopecia in Zdhhc13^{skc4} mice

To study alopecia in detail, we examined hair growth patterns over time by collecting images every 4 days from postnatal day 7 (PND7) to PND67. Before PND11, the appearance of body hair did not differ between homozygous Zdhhc13^{skc4} mice (Figure 1a) and wild-type (WT) littermates. With time, affected mice began to exhibit dry, frizzy, lusterless hair in contrast to the supple, smooth, glossy hair on WT littermates. Hair loss from the head began at PND19, and full-body hair loss was complete at PND27. This growth and loss pattern was repetitive occurring over a 20-day cycle until the affected mice died around the age of 1 year. Cyclic hair loss occurred in both males and females. To investigate the process of hair loss in Zdhhc13^{skc4} hair follicles, we examined mid-dorsal skin histology between PND13 and PND21. Hair growth occurs over a three-stage cycle: growth (anagen), regression (catagen), and resting phase (telogen; Alonso and Fuchs, 2006). Normally, onset of the first catagen ranges from PND14 at the upper back near the head to PND18 at the lower back near the tail; the first telogen occurs from approximately PND19 to PND21 at the mid-back, consistent with observations in both sets of mice (Zdhhc13^{skc4} and WT; Supplementary Figure S1 online). Importantly, we saw no phase delay in the Zdhhc13^{skc4} mice, and hair loss occurred at the telogen phase.

Defective CUH and hair anchoring

We examined the anchoring structures of hair from the lower back at 23 days of age. On scanning electron microscopy, homozygous Zdhhc13^{skc4} mice exhibited a ragged and dilapidated cuticle of hair shaft (CUH) in contrast to WT and heterozygous mice that showed a smooth CUH (Figure 1b). On transmission electron microscopy, some areas of the hair cuticle were irregular in shape and stripped off from the hair shaft (Supplementary Figure S2b online, arrow). The hair sheath was also separated from the hair shaft in the defective region of the affected mice. Hair club structure, however, appeared normal in the homozygous Zdhhc13^{skc4} mice (Supplementary Figure S3a online). In the hair-pull test, the number of pulled-out hairs per square centimeter of adhesive tape was significantly greater in homozygous Zdhhc13^{skc4} mice (28.7 ± 3) than in WT (5.3 ± 0.7) and heterozygous (2.8 ± 0.7) mice at 21 days of age (Figure 1c and d). The results revealed poor hair anchoring with a defective CUH structure.

Hyperproliferation and disorganized cornification of keratinocytes in Zdhhc13^{skc4} mice

We previously reported hyperkeratosis in the epidermis of Zdhhc13^{skc4} mice at 16 weeks of age (Saleem *et al.*, 2010). The phenotype was also found in homozygous affected mice as early as PND7 (Supplementary Figure S4 online). Furthermore, acanthosis and thicker stratum lucidum were observed in the homozygous affected mice as early as PND1 (Supplementary Figure S4 online). On transmission electron microscopy, the number of cornified layers in the affected epidermis was increased. The cornified layers were generally thicker, and the spaces between them were increased in the homozygous mice compared with those in the WT mice (Supplementary Figure S2a online). To examine hyperkeratosis in greater detail, we used keratin (KE) markers to investigate the skin abnormality. KE6 is a proliferation marker that is normally expressed only in the hair follicle; KEs 10 and 14 are markers of the spinous and granular layers and the basal layer of the epidermis, respectively. However, these KE markers were expressed in the affected mice in all layers of the epidermis, including the cornified layer (Figure 2a, arrows), indicating generalized keratinocyte hyperproliferation and disorganized cornification.

Impaired skin barrier function and a fragile cornified envelope in Zdhhc13^{skc4} mice

The skin is an anatomical barrier and is the first line of defense against foreign invasion. Once this barrier is disrupted, keratinocyte proliferation increases to form a thicker cornified layer (hyperkeratosis) as a physical compensation for the impaired skin barrier. We used PND0 mice to investigate skin barrier function by the toluidine blue dye penetration assay. The skin of the homozygous affected mice was stained with toluidine blue almost throughout the body, whereas that of the WT mice was not (Figure 2b). Thus, the skin barrier function was impaired in the homozygous Zdhhc13^{skc4} mice. In the histological examination, part of the stratum corneum of the mutant skin was fragmentary at PND11 (Supplementary Figure S4 online, left panel, arrow), suggesting impaired toughness of the layer. The toughness of the cornified envelope (CE), an important skin barrier structure that protects

against mechanical stress, was examined by a sonication-shattering assay. At each sonication time point, the percentage of intact CE was significantly lower in the homozygous affected group than in the WT group (Figure 2d). Thus, CEs in homozygous affected mice were fragile and had poor resistance against physical stress.

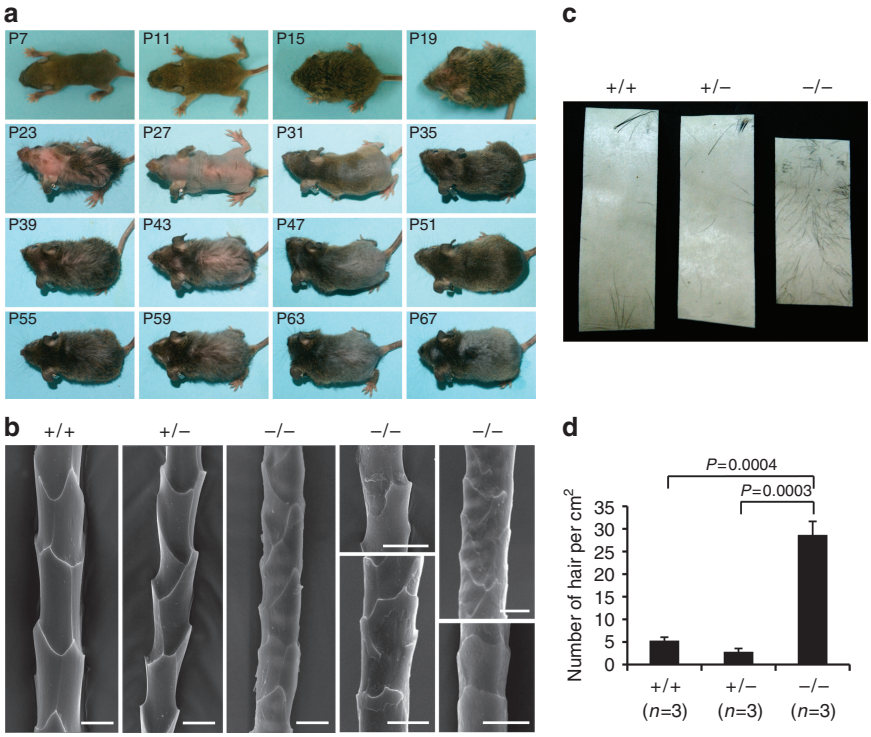

Figure 1. Hair abnormalities in Zdhhc13^{skc4} mice. (**a**) Body hair appearance in the same homozygous affected mouse every 4 days from postnatal day 7 (PND7) to PND67. (**b**) Hair shaft cuticle structure was examined by scanning electron microscopy in wild-type (WT; +/+), heterozygous (+/−), and homozygous affected (−/−) mice. Hairs were taken from the lower back at 23 days of age. Bar = 10 μm. (**c**) Hair-pull test: adhesive tape was applied from head to buttock. (**d**) Quantification of separated hair. Means ± SD are shown. $n = 3$ in each group. P, postnatal day.

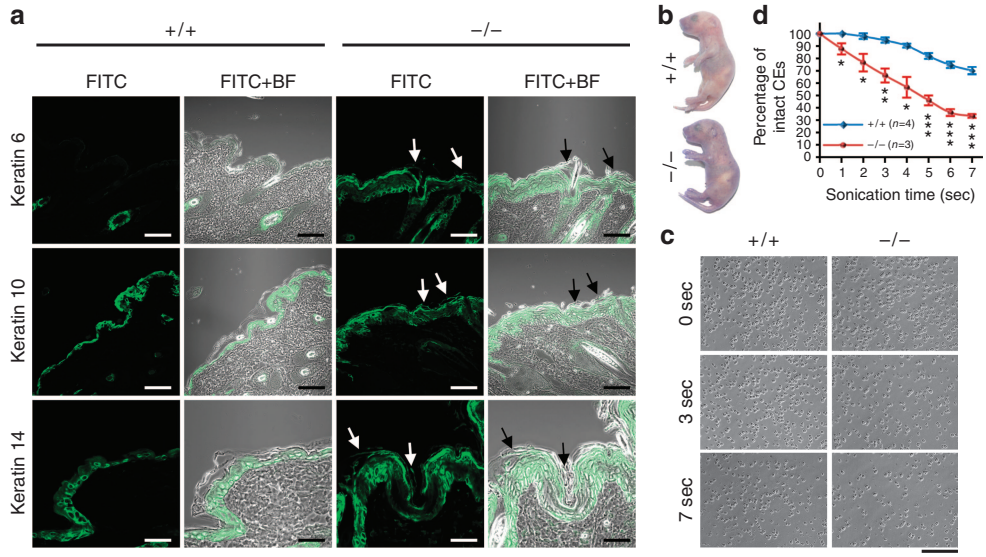

Figure 2. Skin abnormalities in Zdhhc13^{skc4} mice. (**a**) Keratin expression in the skin of Zdhhc13^{skc4} mice. Keratins 6, 10, and 14 were expressed in all layers of the epidermis in homozygous affected mice (−/−) at 4 weeks of age including the cornified layer (arrows); wild type (WT; +/+). Bar = 40 μm (keratins 6 and 10), 10 μm (keratin 14). (**b**) Skin permeability in newborn mice as shown by toluidine blue staining. (**c**) Representative micrographs of cornified envelops (CEs) of mice at PND0 sonicated (1–7 seconds) and examined by a phase microscopy. Bar = 200 μm. (**d**) The percentage of intact CEs in different sonication time groups (1–7 seconds) relative to the untreated group (0 seconds). Means ± SD are shown; *P*-value, * < 0.01, ** < 0.001, and *** < 0.0001 (**d**). BF, bright field.

Table 1. A candidate substrate of DHHC13, cornifelin

Protein name	Peptide sequence	Start position	End position	WT1 – HA	WT1 +HA	WT2 +HA	WT3 +HA	M1 – HA	M1 +HA	M2 +HA	M3 +HA
Cornifelin	ISDDFGE**C**CCAPYLPGGLHSLR	51	72	0	537	455	1,355	0	0	0	0
Cornifelin	ISDDFGEC**C**CAPYLPGGLHSLR	51	72	0	536	454	1,355	0	0	0	0
Cornifelin	ISDDFGECC**C**APYLPGGLHSLR	51	72	0	537	455	1,356	0	0	0	0
Cornifelin	ISDDFGEC**CC**APYLPGGLHSLR	51	72	0	57	41	78	0	0	0	0
Cornifelin	ISDDFGE**CCC**APYLPGGLHSLR	51	72	0	98	22	69	0	0	0	0
Cornifelin	YHIQGSVGHDWAALTF**C**LPCALCQMAR	79	105	0	37	49	156	0	0	0	0
Cornifelin	YHIQGSVGHDWAALTFCLPCAL**C**QMAR	79	105	0	37	49	156	0	0	0	0

Abbreviation: HA, hydroxylamine; WT, wild type.
Cornifelin was identified as a candidate DHHC13 substrate by the ABE-proteomic approach. The numbers in the columns labeled – – HA and +HA represent the number of biotinylated cornifelin peptides. HA-treated groups of three WT (the column of WT1 +HA, WT2 +HA, and WT3 +HA) and three homozygous affected mice at 4 weeks of age (columns M1 +HA, M2 +HA, and M3 +HA). Negative controls are the HA-untreated groups from WT (WT1 –HA) and homozygous *Zhddc13*-deficient mice (M1 –HA). The bold and underlined "C" in the column Peptide sequence is the biotinylated cysteine representing the palmitoylated site; Start position and End position represent the position of the first and last amino acid of the biotinylated cornifelin peptide fragment.

Cornifelin as a candidate substrate of DHHC13

To investigate the molecular mechanism by which DHHC13, a Palmitoylation enzyme, results in skin and hair abnormalities, we examined putative DHHC13 substrates. We compared the Palmitoylation levels of skin proteins in three WT and three affected mice at 4 weeks of age by using the acyl-biotinyl exchange (ABE)-proteomic approach. Palmitate in the putative PAT substrates was substituted with biotin. Candidate proteins with decreased or no Palmitoylation in Zdhhc13^{skc4} skin were identified as putative DHHC13 substrates. Using mass spectrometry analysis, we identified several candidate substrates without any Palmitoylation signal in the mutant skins. Among these substrates, the most striking one was cornifelin (Table 1), encoded by the *Cnfn* gene. This was evidenced by the fact that cornifelin has the greatest numbers of Palmitoylation sites and the highest S-Palmitoylation signal in the WT skins. The cornifelin had none-to-all S-Palmitoylation signal on five cysteines (presenting on two peptides, ISDDFGEC^{58}C^{59}C^{60}APYLPGGLHSLR and YHIQGSVGHDWAALTFC^{95}LPCALC^{101}QMAR) in all of the three WT skins, and these S-palmitoylated peptides were completely absent in all of the three Zdhhc13^{skc4} skins. The result indicated that cornifelin contains five palmitoylated cysteines and is a specific PAT substrate of DHHC13.

Absence of cornifelin protein in the skin and hair of Zdhhc13^{skc4} mice

Our *in situ* hybridization experiments showed that *Zdhhc13* mRNA was normally expressed in the epidermis and hair follicles of the skin of the WT mice (Supplementary Figure S5 online). Cornifelin, highly expressed in the horny cell layer (cornified layer) of human skin, was identified as a novel component of the CE in 2004 (Michibata *et al.*, 2004). In mice, cornifelin was expressed primarily in the granular and cornified layers of the epidermis (Figure 3a). In the hair follicle, cornifelin was colocalized with KE72 (Figure 3b, top panel) and part of KE82 (Figure 3b bottom panel, arrows), indicating that cornifelin was expressed in the cuticle of the inner root sheath (Cui) and the surface layer of CUH. Cornifelin was undetectable in the epidermis and hair follicle of homozygous Zdhhc13^{skc4} mice at 4 weeks of age (Figure 3a). Loss of cornifelin in the affected skin was also confirmed by western blotting (Figure 3c). Interestingly, the mRNA expression level of *Cnfn* was significantly higher in the affected skin than in the WT skin ($P=0.016$), whereas the *Zdhhc13* mRNA expression level was significantly lower in the affected skin than in the WT skin ($P=0.001$; Figure 3d).

DHHC13 palmitoylates cornifelin

As shown in Table 1, the ABE-proteomic approach identified cornifelin as a candidate DHHC13 substrate because of the absence of biotinylated peptides in the skin of homozygous affected mice. However, this result could also be due to the absence of cornifelin. To ensure that cornifelin is indeed a substrate of DHHC13, we co-transfected HEK293T cells with cornifelin-myc and a Flag vector, WT, or a mutated DHHC13-Flag (a truncated form of DHHC13 that mimics the nonsense mutation of *Zdhhc13* gene in our mouse model; Figure 4a). Immunoprecipitation with anti-myc antibody and the ABE assay clearly showed higher cornifelin-myc Palmitoylation levels in the WT DHHC13-Flag group than in the Flag vector group (basal Palmitoylation level from endogenous PATs of HEK293T cells) or the mutant DHHC13-Flag group (Figure 4b). In fact, mutant DHHC13 could not palmitoylate cornifelin, as its level was similar to that of the Flag vector control.

Palmitoylation of Cys95 and Cys101 is required for cornifelin expression

To investigate the effect of each of the five palmitoylated cysteines on cornifelin, each residue was substituted with serine by site-directed mutagenesis. We generated a collection of cornifelin-myc constructs including single-site mutations (C58S, C59S, C60S, C95S, and C101S), four-site mutations (C59-60-95-101S, C58-60-95-101S, C58-59-95-101S, C58-59-60-101S, and C58-59-60-95S), and a full five-site mutation. As shown in Figure 5, expression of cornifelin-myc was significantly reduced in C95S ($P<10^{-7}$) and C101S ($P<10^{-3}$) compared with the WT, whereas there

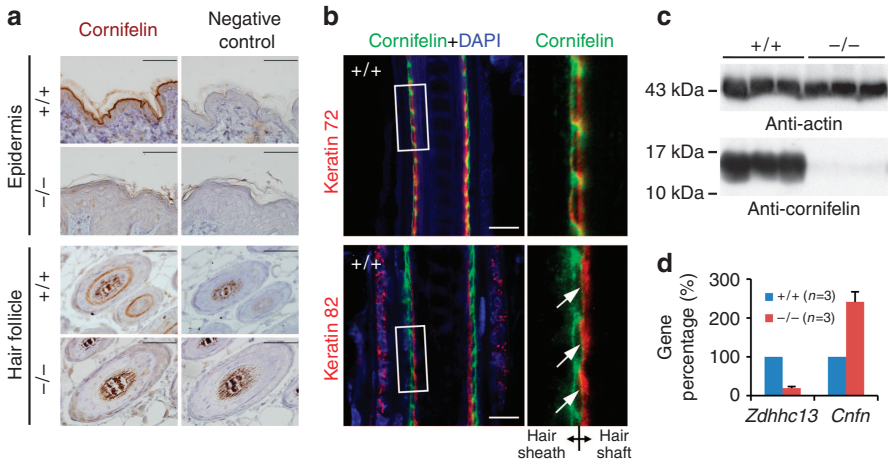

Figure 3. Expression of cornifelin in the skin and hair of Zdhhc13^{skc4} mice. (**a**) Expression of cornifelin in the epidermis and hair follicle (cross section) of wild-type (WT; +/+) and homozygous affected (−/−) mice at 4 weeks of age. IHC, Bar = 50 μm. (**b**) Cornifelin (green), keratin 72 (red), keratin 82 (red), and DAPI (blue) in the hair follicle (vertical section) of a WT mouse at 4 weeks of age. The right panels are the enlarged image from the boxed area on the left panels. Bar = 10 μm. (**c**) Immunoblotting of cornifelin and actin in the skins of mice at 4 weeks of age. (**d**) Gene expression of *Zdhhc13* and *cnfn* was assessed by qPCR in the skins of mice at 4 weeks of age.

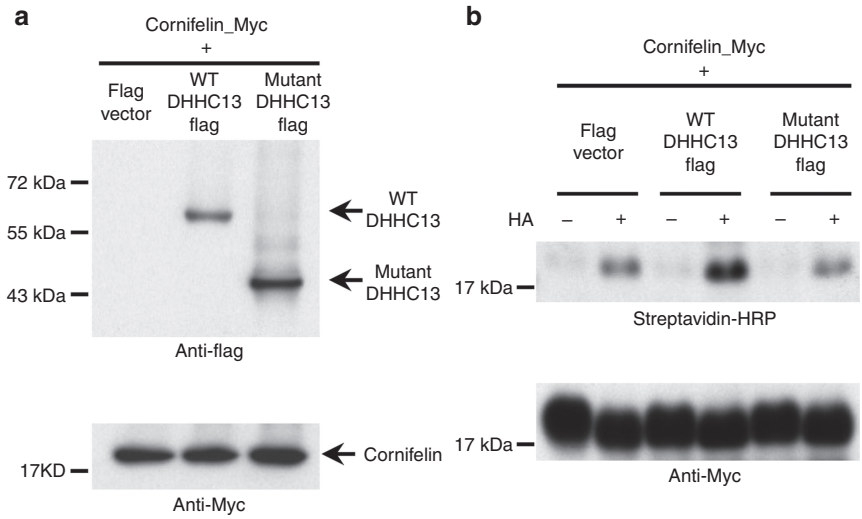

Figure 4. Analysis of palmitoylation specificity of DHHC13 for cornifelin. HEK293T cells were co-transfected with cornifelin-myc and Flag vector (group 1), wid type (WT; group 2), or the mutant DHHC13-Flag (group 3) for 24 hours. (**a**) Expression of cornifelin and DHHC13 (WT and mutant) in each co-transfection group. (**b**) Palmitoylation of cornifelin. The co-overexpression groups were immunoprecipitated with myc antibody and followed by the acyl-biotinyl exchange (ABE) assay. During ABE, each co-transfected group was divided into –HA (hydroxylamine; negative control) and +HA (treat with and without HA) subgroups. The amount and biotinylation levels of purified cornifelin in each group were detected with anti-myc antibody and streptavidin-horseradish peroxidase, respectively.

was no significant change in C58S, C59S, and C60S. The importance of Cys95 and Cys101 for cornifelin protein expression was confirmed by the 4- and 5-site mutations (Figure 5). There was no significant change in RNA expression in the mutant groups versus WT.

DISCUSSION

In this study, Zdhhc13^{skc4} mice exhibited a ragged and dilapidated CUH and a poor hair anchoring ability that resulted in cyclic alopecia. In the skin, the disturbed cornification and fragile CE affected skin barrier function and resulted in hyperkeratosis.

Cyclic alopecia has been reported in other mouse models including *Sox21*, *Msx2* knockout, and the repeated epilation of heterozygous (*Er*/+) mice (Ma *et al.*, 2003; Kiso *et al.*, 2009; Xin *et al.*, 2010). Sox21 is expressed in the cuticle layer and progenitor cells of the hair shaft in mice and is required for hair cuticle formation. Absence of *Sox21* causes loss of the interlocking structures of the hair cuticle. Loss of *Msx2* in mice causes defects in hair cycling and differentiation, which resulted in the structural hair shaft abnormalities. *Er*/+ mice containing one allele expressing a dominant-negative 14-3-3σ mutant protein exhibited a depauperated club of hair. All mice with cyclic alopecia, including ours, exhibited a defect

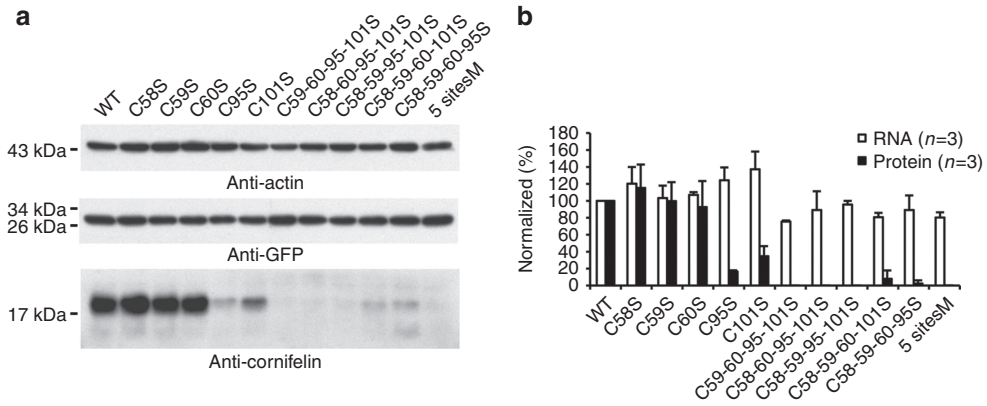

Figure 5. RNA and protein expression. (**a**) Immunoblot analysis of each cornifelin mutant. The cornifelin-myc constructions included single-site mutants (C58S, C59S, C60S, C95S, and C101S), four-site mutants (C59-60-95-101S, C58-60-95-101S, C58-59-95-101S, C58-59-60-101S, and C58-59-60-95S), and a five-site mutant (5 sites M). XB2 cells were co-transfected with equal amounts of plasmid DNA encoding cornifelin-myc and GFP (as a control for transfection efficiency). Actin was used as a loading control. (**b**) Cornifelin expression was quantified and normalized to GFP. The percent normalized RNA or protein for each mutation is expressed relative to wild type (WT). $n = 3$ in each group.

in the hair anchoring structures affecting either the hair cuticle or the hair club. Our Zdhhc13^{skc4} mice had ragged and dilapidated hair cuticles but normal hair clubs. The hair cuticle defect in our mice most closely resembles that of *Sox21*-null mice. However, the location and expression of Sox21 were normal in our Zdhhc13^{skc4} mice (Supplementary Figure S3b online). This suggests that the hair cuticle defect in our Zdhhc13^{skc4} mice is independent of the mechanism in Sox21-null mice.

Our Zdhhc13^{skc4} mice also exhibited a fragile CE, an essential structure for the skin barrier. It is an insoluble, highly compact protein layer adjacent to the interior surface of the plasma membrane of the differentiated keratinocyte (Nemes and Steinert, 1999). During CE formation, transglutaminases (TG)1, TG3, and TG5 cross-link the CE components such as involucrin, loricrin, SPR, envoplakin, and periplakin (Candi *et al.*, 2005). Defects of TG1 or CE components caused CE absence or fragility, which resulted in skin barrier dysfunction in TG1-null mice and the triple-knockout mice (envoplakin$^{-/-}$; involucrin$^{-/-}$; periplakin$^{-/-}$; Kuramoto *et al.*, 2002; Sevilla *et al.*, 2007). However, none of these mouse models have cyclic alopecia. In addition, expression of involucrin in keratinocyte and hair follicle cells was normal in our Zdhhc13^{skc4} mice (Supplementary Figure S6b online).

Zdhhc21^{dep} mice (MGI:1856841), which is another PAT-deficient mouse model, exhibited hair and skin abnormalities, including alopecia and hyperplasia of the interfollicular epidermis and sebaceous glands (Mill *et al.*, 2009). However, in the Zdhhc21^{dep} mice, hair loss was mild, without a cyclic pattern, and the hair follicle differentiation was delayed. These features are different from those of our Zdhhc13^{skc4} mice, in which severe and cyclic alopecia and normal hair cycle were observed.

In this study, we found that cornifelin is a specific substrate of DHHC13 and was absent in the hair follicle and epidermis of our Zdhhc13^{skc4} mice; specifically, cornifelin was absent in the CUH and CE structures. Cornifelin has been garnered attention in recent years for its increased expression in psoriatic skin. In the epidermis, cornifelin is a component of the CE and is cross-linked to at least two other CE proteins—involucrin and loricrin (Michibata *et al.*, 2004). However, the function of cornifelin remains unclear because of a lack of functional studies. We therefore propose that cornifelin has an important role in the skin barrier and hair anchoring because of its unique localization. Our primary culture experiment demonstrated the translocation of cornifelin from the perinucleus to the cytosol and finally to the plasma membrane where the CE is attached (Supplementary Figure S6a online). In the hair, our immunofluorescence study revealed that cornifelin expressed in the outer layer of the cuticle of the hair shaft contains a highly cross-linked protein layer—the A-layer. Similar to the role of CE in the epidermis, the A-layer provides considerable mechanical toughness, chemical resilience, and physical protection (Wei and Bhushan, 2006). On the basis of these results, we suggest that the loss of cornifelin caused the ragged and dilapidated CUH and poor hair anchoring ability, which resulted in cyclic alopecia. In the skin, the disturbed cornification and fragile CE affected the skin barrier function and resulted in hyperkeratosis. Direct evidence of a causal relationship between cornifelin in the hair and skin abnormalities now awaits the generation of a *cnfn*-deficient mouse.

However, the mechanisms by which DHHC13 deficiency and defective cornifelin Palmitoylation result in loss of cornifelin are not clear. The absence of cornifelin protein was not due to silencing (no expression) of *cnfn*. mRNA expression of *Cnfn* increased in the skin of Zdhhc13^{skc4} mice compared with the WT. It is also unlikely to be due to ENU induction of another mutation in *Cnfn*, as cornifelin was also absent in the Zdhhc13Gt(AC0492)^{Wtsi} mice (a gene trap mouse model, MGI: 4338023; Supplementary Figure S7 online). Furthermore, cornifelin was lost in primary keratinocyte and hair follicle cell cultures derived from the skin of affected mice (Supplementary Figure S6b online), suggesting that the loss of cornifelin was a primary effect of *Zdhhc13* deficiency, not a secondary effect, such as inflammation or

infection (see Supplementary information online for more detailed discussion). Interestingly, removing the Palmitoylation of Cys95 or C101 by mutating the cysteine to serine at these positions markedly reduced the amount of cornifelin protein, suggesting that Palmitoylation was essential for cornifelin protein stability. However, a proteasome inhibitor, MG132, and/or a Protease Inhibitor Cocktail (Sigma-Aldrich, St Louis, MO, P 1860) did not increase the protein amount (data not shown), suggesting that the loss of cornifelin due to the absence of Palmitoylation was not due to protein degradation. Further research is needed to elucidate the mechanism by which defective Palmitoylation resulted in the loss of cornifelin.

To our knowledge, this is the first study to demonstrate that PAT is important for maintaining normal CUH and CE structure and normal hair anchoring and skin barrier function. This phenomenon is likely mediated by cornifelin, a component of CUH and CE and a key substrate of DHHC13. In conclusion, our study revealed an important role for cornifelin, a Palmitoylation substrate, in cyclic alopecia and skin abnormality in Zdhhc13^{skc4} mice.

MATERIALS AND METHODS

Mouse model

Zdhhc13^{skc4} mice with a nonsense *Zdhhc13* mutation (c.1273A>T) induced by ENU mutagenesis were generated in the C57BL/6*129S6/SvEvTac*C3H genetic background as described previously (Saleem *et al.*, 2010). All of the mice were housed under a controlled temperature and a humid environment in a clean and specific pathogen-free room with a healthy breeding colony. Genomic DNA from mice tails was extracted with the Gentra Puregene kit (Qiagen, Hilden, Germany, D-50K). All animal experiments complied with the animal protocol approved by institutional animal care and use committees (Academia Sinica, Taiwan).

Scanning electron microscopy

Mouse hair samples were attached to aluminum mounts with carbon adhesive tabs, coated with gold, and analyzed by scanning electron microscopy (JEOL JSM T330A).

Histology and immunostaining

Mouse skin samples were fixed in 4% paraformaldehyde (pH 7.4) and embedded in paraffin wax. The paraffin sections were stained with hematoxylin and eosin. Rabbit polyclonal anti-mouse cornifelin (produced by LTK BioLaboratories, Taoyuan, Taiwan) and anti-rabbit horseradish peroxidase–conjugated secondary antibody (Vectastain ABC systems, Vector Laboratories, Servion, Switzerland) were utilized for immunohistochemistry. Rabbit polyclonal anti-mouse cornifelin (LTK BioLaboratories), rabbit polyclonal anti-mouse KE6, 10, and 14 (Covance, Berkeley, CA; PRB-169P, PRB-159P, and PRB-155P), guinea pig polyclonal anti-mouse KE72 and 82 (Progen Biotechnics, Heidelberg, Germany; FRG, GP-K6irs2, and GP-hHb2), goat polyclonal anti-mouse SOX21 (Neuromics, Bloomington, MN; GT15209) and anti-mouse Alexa Fluor 488, anti-guinea pig Alexa Fluor 594, and anti-goat Alexa Fluor 594–conjugated secondary antibodies (Life Technologies, Gaithersburg, MD, A-11001, A-11076 and A-11058), and DAPI (Invitrogen, Grand Island, NY) were utilized for immunofluorescence.

Gene expression analysis

Total RNA was extracted from XB2 cells or mouse skins by using the RNeasy kit (Qiagen; 74136) according to the manufacturer's protocols. cDNA synthesized with the SuperScript III First-Strand Synthesis Kit (Invitrogen; 18080-051) was used as the template in qPCR with Power SYBR green PCR Master Mix (Applied Biosystems, Foster City, CA; 4367659) on an ABI PRISM 7700 Sequence Detection System or a ViiA 7 Real-Time PCR System (Applied Biosystems). Primers of qPCR are listed in Supplementary Table S1 online.

Skin permeability assay and analysis of CEs

The skin permeability assay was performed with toluidine blue as described (Kuramoto *et al.*, 2002). CEs were isolated from the dorsal skin of newborn mice as described (Koch *et al.*, 2000). For sonication, CEs were suspended in 2% SDS buffer. CEs were sonicated in a cup sonicator (Misonix Sonicator 3000, Misonix, Inc., Farmingdale, NY) at 4 °C for various time points. Intact CEs were counted by using a hemocytometer. Bright-field images were captured on an inverted microscope (AxioVert.A1; Zeiss).

Western blot

Western blotting was performed as described (Song *et al.*, 2014). Primary antibodies included rabbit polyclonal anti-cornifelin (LTK BioLaboratories), mouse monoclonal anti-Actin (Millipore, Billerica, MA; MAB1501, 1:20,000), mouse monoclonal anti-myc (Millipore; 05-724, 1:1,000), mouse monoclonal anti-FLAG (Sigma-Aldrich; F1804, 1:1,000), and mouse monoclonal anti-GFP (Millipore; MAB3580, 1:1,000). horseradish peroxidase–conjugated goat anti-mouse and goat anti-rabbit secondary antibodies (Millipore; AP124P and AP132P, 1:5,000) were applied to the primary antibodies.

Proteomic analysis of skin protein S-Palmitoylation (ABE-proteomic approach)

Extraction of membrane protein from the skins of the mice and the ABE assay were performed as described (Wan *et al.*, 2007; Chen *et al.*, 2010) with several modifications. First, skin protein extracts in 4% SDS buffer were reduced in 5 mM tris(2-carboxyethyl)phosphine (Sigma-Aldrich) at 37 °C for 30 minutes and incubated with 200 mM iodoacetamide (Sigma-Aldrich) in 20 mM HEPES/5% (w/v) SDS at 37 °C for 2 hours in the dark. After acetone precipitation to remove excess iodoacetamide and washing three times with 95% ice-cold ethanol, protein pellets were resuspended in HEN buffer containing 1% SDS. EZ-Link iodoacetyl-PEG2-biotin (2 mM; Pierce, Rockford, IL) was added with or without 0.7 M hydroxylamine and reacted at 37 °C for 2 hours in the dark. After removing excess hydroxylamine and biotin by acetone precipitation, the protein pellets were resuspended in profiling buffer (50 mM Tris at pH 8.3, 0.1% (w/v) SDS, 0.02% (w/v) Triton X-100, and 2 M urea). For mass spectrometry, 1.5 mg of the biotinylated protein was diluted with Milli-Q water to a final concentration of 1 M urea, digested with trypsin (1:25 w/w; trypsin/proteins) at 37 °C for 16 hours, and dried completely under vacuum. The biotinylated peptides were enriched by streptavidin agarose (Sigma-Aldrich), desalted by C18 Zip-tip (Millipore), and then analyzed by mass spectrometry and label-free quantitation.

Construction and mutagenesis

WT and mutant *Zdhhc13* cDNA were subcloned into the p3XFLAG-CMV14 vector (Sigma-Aldrich). *Cnfn* cDNA was subcloned into the

pcDNA4/myc-His expression vector (Invitrogen). Primers of cloning are listed in Supplementary Table S1 online. Palmitoylated cysteines of cornifelin-myc were mutated to serine by QuikChange Lightning Site-Directed Mutagenesis (Agilent Technologies, Palo Alto, CA; #200518). Primers used in site-directed mutagenesis are listed in Supplementary Table S1 online.

ABE assay

HEK293T cells were co-transfected with cornifelin-myc and Flag vector, WT, or the mutant of DHHC13-Flag for 24 hours. Collected cells were lysed in buffer (LB: 150 mM NaCl, 50 mM Tris-HCl, 5 mM EDTA, 1 mM PMSF, 1× protease inhibitor (Roche, Indianapolis, IN), 1% Triton X-100, pH 7.4) containing 50 mM N-ethylmaleimide (Sigma-Aldrich). Cornifelin was immunoprecipitated with mouse anti-Myc antibody (Millipore, 1:250) followed by the ABE assay as described previously (Huang *et al.*, 2009) with modification. Biotin labeling of cornifelin was performed with saturated biotin-BMCC solution (in LB).

Statistical analysis

Student's *t*-test was used for all comparisons. A *P*-value of <0.05 was considered statistically significant.

CONFLICT OF INTEREST

The authors state no conflict of interest.

ACKNOWLEDGMENTS

This study was supported by the Academia Sinica Genomic Medicine Multicenter Study (40-05-GMM) and Ministry of science and technology, Taiwan (National Center for Genome Medicine, Most 103-2319-B-001-001). Taiwan Mouse Clinic (MOST 103-2325-B-001-015) funded by the National Research Program for Biopharmaceuticals (NRPB) at the Ministry of Science and Technology (MOST) of Taiwan. We thank the Sequencing Core Facility at the Scientific Instrument Center at Academia Sinica for DNA sequencing and the Pathology Core Lab of IBMS at Sinica for the histology and SEM and TEM technical support.

SUPPLEMENTARY MATERIAL

Supplementary material is linked to the online version of the paper at http://www.nature.com/jid

REFERENCES

Alonso L, Fuchs E (2006) The hair cycle. *J Cell Sci* 119:391–3

Bartels DJ, Mitchell DA, Dong X *et al.* (1999) Erf2, a novel gene product that affects the localization and palmitoylation of Ras2 in *Saccharomyces cerevisiae*. *Mol Cell Biol* 19:6775–87

Berchtold LA, Storling ZM, Ortis F *et al.* (2011) Huntingtin-interacting protein 14 is a type 1 diabetes candidate protein regulating insulin secretion and beta-cell apoptosis. *Proc Natl Acad Sci USA* 108:E681–8

Blaskovic S, Adibekian A, Blanc M *et al.* (2014) Mechanistic effects of protein palmitoylation and the cellular consequences thereof. *Chem Phy Lipids* 180:44–52

Candi E, Schmidt R, Melino G (2005) The cornified envelope: a model of cell death in the skin. *Nat Rev Mol Cell Biol* 6:328–40

Charollais J, Van Der Goot FG (2009) Palmitoylation of membrane proteins (review). *Mol Membr Biol* 26:55–66

Chen YJ, Ku WC, Lin PY *et al.* (2010) S-alkylating labeling strategy for site-specific identification of the s-nitrosoproteome. *J Proteome Res* 9:6417–39

Fukata M, Fukata Y, Adesnik H *et al.* (2004) Identification of PSD-95 palmitoylating enzymes. *Neuron* 44:987–96

Grantham ML, Wu WH, Lalime EN *et al.* (2009) Palmitoylation of the influenza A virus M2 protein is not required for virus replication *in vitro* but contributes to virus virulence. *J Virol* 83:8655–61

Huang K, Sanders S, Singaraja R *et al.* (2009) Neuronal palmitoyl acyl transferases exhibit distinct substrate specificity. *FASEB J* 23:2605–15

Iwanaga T, Tsutsumi R, Noritake J *et al.* (2009) Dynamic protein palmitoylation in cellular signaling. *Prog Lipid Res* 48:117–27

Kiso M, Tanaka S, Saba R *et al.* (2009) The disruption of Sox21-mediated hair shaft cuticle differentiation causes cyclic alopecia in mice. *Proc Natl Acad Sci USA* 106:9292–7

Koch PJ, de Viragh PA, Scharer E *et al.* (2000) Lessons from loricrin-deficient mice: compensatory mechanisms maintaining skin barrier function in the absence of a major cornified envelope protein. *J Cell Biol* 151:389–400

Korycka J, Lach A, Heger E *et al.* (2012) Human DHHC proteins: a spotlight on the hidden player of palmitoylation. *Eur J Cell Biol* 91:107–17

Kuramoto N, Takizawa T, Takizawa T *et al.* (2002) Development of ichthyosiform skin compensates for defective permeability barrier function in mice lacking transglutaminase 1. *J Clin Invest* 109:243–50

Ma L, Liu J, Wu T *et al.* (2003) 'Cyclic alopecia' in Msx2 mutants: defects in hair cycling and hair shaft differentiation. *Development* 130:379–89

Michibata H, Chiba H, Wakimoto K *et al.* (2004) Identification and characterization of a novel component of the cornified envelope, cornifelin. *Biochem Biophys Res Commun* 318:803–13

Mill P, Lee AW, Fukata Y *et al.* (2009) Palmitoylation regulates epidermal homeostasis and hair follicle differentiation. *PLoS Genet* 5:e1000748

Milnerwood AJ, Parsons MP, Young FB *et al.* (2013) Memory and synaptic deficits in Hip14/DHHC17 knockout mice. *Proc Natl Acad Sci USA* 110: 20296–301

Nemes Z, Steinert PM (1999) Bricks and mortar of the epidermal barrier. *Exp Mol Med* 31:5–19

Ohno Y, Kihara A, Sano T *et al.* (2006) Intracellular localization and tissue-specific distribution of human and yeast DHHC cysteine-rich domain-containing proteins. *Biochim Biophys Acta* 1761:474–83

Roth AF, Feng Y, Chen L *et al.* (2002) The yeast DHHC cysteine-rich domain protein Akr1p is a palmitoyl transferase. *J Cell Biol* 159:23–8

Rousso I, Mixon MB, Chen BK *et al.* (2000) Palmitoylation of the HIV-1 envelope glycoprotein is critical for viral infectivity. *Proc Natl Acad Sci USA* 97:13523–5

Saleem AN, Chen YH, Baek HJ *et al.* (2010) Mice with alopecia, osteoporosis, and systemic amyloidosis due to mutation in Zdhhc13, a gene coding for palmitoyl acyltransferase. *PLoS Genet* 6:e1000985

Sevilla LM, Nachat R, Groot KR *et al.* (2007) Mice deficient in involucrin, envoplakin, and periplakin have a defective epidermal barrier. *J Cell Biol* 179:1599–612

Singaraja RR, Hadano S, Metzler M *et al.* (2002) HIP14, a novel ankyrin domain-containing protein, links huntingtin to intracellular trafficking and endocytosis. *Hum Mol Genet* 11:2815–28

Singaraja RR, Huang K, Sanders SS *et al.* (2011) Altered palmitoylation and neuropathological deficits in mice lacking HIP14. *Hum Mol Genet* 20: 3899–909

Song IW, Li WR, Chen LY *et al.* (2014) Palmitoyl acyltransferase, Zdhhc13, facilitates bone mass acquisition by regulating postnatal epiphyseal development and endochondral ossification: a mouse model. *PloS One* 9:e92194

Sutton LM, Sanders SS, Butland SL *et al.* (2013) Hip14l-deficient mice develop neuropathological and behavioural features of Huntington disease. *Hum Mol Genet* 22:452–65

Wan J, Roth AF, Bailey AO *et al.* (2007) Palmitoylated proteins: purification and identification. *Nat Protoc* 2:1573–84

Wei G, Bhushan B (2006) Nanotribological and nanomechanical characterization of human hair using a nanoscratch technique. *Ultramicroscopy* 106: 742–54

Xin Y, Lu Q, Li Q (2010) 14-3-3sigma is required for club hair retention. *J Investig Dermatol Symp Proc* 130:1934–6

Yanai A, Huang K, Kang R *et al.* (2006) Palmitoylation of huntingtin by HIP14 is essential for its trafficking and function. *Nat Neurosci* 9:824–31

Yu L, Reader JC, Chen C *et al.* (2011) Activation of a novel palmitoyltransferase ZDHHC14 in acute biphenotypic leukemia and subsets of acute myeloid leukemia. *Leukemia* 25:367–71